Journal of Structural Geology, Vol. 15, No. 2, pp. 145 to 161, 1993
Printed in Great Britain

0191-8141/93 $06.00+0.00

Offscraping accretion of Jurassic chert–clastic complexes in the Mino–Tamba Belt, central Japan

KATSUMI KIMURA

Department of Geology, Geological Survey of Japan, Tsukuba 305, Japan

and

RIE HORI

Department of Earth Sciences, Faculty of General Education, Ehime University, Matsuyama 790, Japan

(*Received* 15 *October* 1991; *accepted in revised form* 14 *July* 1992)

Abstract—Detailed structural and biostratigraphical analysis of the Jurassic Inuyama Sequence, a coherent chert–clastic complex in the Mino–Tamba Belt, central Japan, clarifies the evolution of accretionary processes at shallow structural levels. The Inuyama Sequence is characterized by a series of stacked thrust sheets. Each sheet consists of an Early Triassic to Middle Jurassic oceanic plate stratigraphy composed of four lithologic units which are, in ascending order: siliceous claystone; ribbon chert; siliceous mudstone; and clastic rocks. The structural features of the Inuyama Sequence demonstrate a four-stage progressive deformation. (1) A décollement was initiated within the siliceous mudstone when this sequence was just seaward of the deformation front. Clastic dikes and sills formed at the horizon just above the décollement at this time. (2) The stratigraphic section above the décollement was imbricated by in-sequence thrusting in the frontal part of the wedge. This initial stage of thrusting and imbrication was followed by (3) the formation of duplex structures with fault-related folds within the lower stratigraphic section as the décollement stepped down-section to the lowest siliceous claystone interval. Finally, (4) these thrust packages were overprinted by secondary prism thickening in the form of out-of-sequence thrust faulting.

INTRODUCTION

CHERT–CLASTIC complexes, which consist of a mixture of clastic rocks and radiolarian chert, have been widely recognized in Phanerozoic circum-Pacific to Tethyan orogenic belts. Detailed biostratigraphic studies of microfossils (e.g. Yao *et al.* 1980, Matsuoka 1984, Murchey 1984, Stewart *et al.* 1986) have contributed significantly to the structural analysis of these orogenic belts. These data demonstrate well the ubiquitous occurrence of layer-parallel thrust faults in the chert–clastic complexes. From modern analogs, the ancient chert–clastic complexes are thought to have formed by tectonic mixing and slicing of oceanic materials (e.g. chert, basalt and limestone) with much younger trench-fill deposits during subduction (e.g. Matsuoka 1984, Taira *et al.* 1989, Matsuda & Isozaki 1991).

Seismic profiling across modern accretionary prisms has made apparent the regional-scale geometric features of thrust systems within prisms and allowed their evolution to be inferred (e.g. Seely *et al.* 1974, Aoki *et al.* 1983, Westbrook *et al.* 1984, Moore *et al.* 1990). The seismically opaque interiors of prisms, however, preclude a clear resolution of structural features. Consequently, in order to answer how accretionary prisms grow at shallow structural levels, ranging from depths of 1 to nearly 10 km, it is very helpful to clarify the structural evolution of exposed ancient accreted rocks by analyzing the detailed geometry of regional-scale thrust systems as well as small-scale structures.

In this paper, we describe the regional-scale structures of a coherent accretionary complex of Jurassic age. This is done using detailed biostratigraphic data and the distinct characteristics of oceanic plate stratigraphy, and also by analysis of small-scale deformational structures. Finally, we present the evolution of the accretionary process, which involves offscraping followed by downstepping of the décollement and out-of-sequence thrusting.

Our studied complex is a part of the Mino–Tamba Belt located near the city of Inuyama, central Japan (Fig. 1). The Mino–Tamba Belt constitutes a major composite accretionary prism that ranges in age from Jurassic to earliest Cretaceous and stretches for over 800 km from the westernmost part of Honshu Island to near Tokyo (e.g. Otsuka 1988, Wakita 1988). The strata in this belt generally dip to the north and consist of imbricated coherent sedimentary units (including turbidite and chert) and melange that young progressively to the south or to structurally lower units (Otsuka 1988, Wakita 1988). Metamorphic studies show that basaltic rocks and adjacent strata suffered regional metamorphism of prehnite–pumpellyite to pumpellyite–actinolite facies (Hashimoto & Saito 1970).

The Mino–Tamba Belt of central Japan can be divided into four tectonostratigraphic units (labelled A,B,C and D from north to south in Fig. 1, which was compiled from Otsuka 1988 and Wakita 1988). The units are separated by N-dipping thrust faults. Units A and B consist of melange characterized by older oceanic

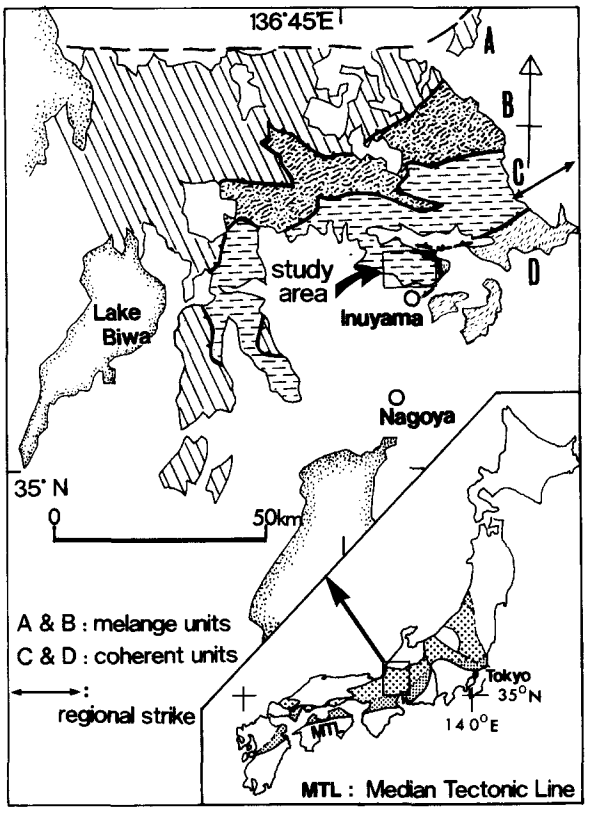

Fig. 1. Simplified geologic map of the Mino–Tamba Belt, central Japan. The Jurassic accretionary complex in the Mino–Tamba Belt and correlative rocks are stippled on the regional inset map, and the southern part (denser stippling) is characterized by low *P–T* metamorphic rocks that make up the Ryoke metamorphic belt. The classification of accretionary complexes in the Mino–Tamba Belt is modified from Otsuka (1988) and Wakita (1989). Unit C is called the Inuyama Sequence in this paper.

materials (e.g. basalt, ribbon chert and limestone) within a younger shale matrix. In contrast, units C and D are coherent sedimentary bodies characterized by stacked thrust sheets composed of ribbon chert, hemipelagite and coarse clastic rocks (e.g. Kido 1982, Otsuka 1988, Wakita 1988). According to recent studies (Otsuka 1988, Wakita 1988), the age of the coarse clastic rocks in these units ranges from Jurassic to earliest Cretaceous, while the pelagic and hemipelagic rocks range in age from Carboniferous to Middle Jurassic. The consistent age relationships of different lithologies allow us to reconstruct an oceanic plate stratigraphy in each tectonic unit. These successions are interpreted to reflect migration of the depocenter from the abyssal plain to the trench floor (e.g. Wakita 1988, Matsuda & Isozaki 1991).

The area studied here occurs in unit C (informally called the Inuyama Sequence) (Fig. 2) and it provides excellent examples of an imbricate thrust system composed of a typical oceanic plate stratigraphy (e.g. Yao *et al.* 1980, Matsuda & Isozaki 1991).

GENERAL GEOLOGY OF THE INUYAMA SEQUENCE

The Inuyama Sequence is approximately 7000 m in structural thickness and composed of a number of stacked fault slices. Among these, regional-scale thrust sheets are identified as bodies that contain an almost complete oceanic plate stratigraphy (Fig. 3). This recon-

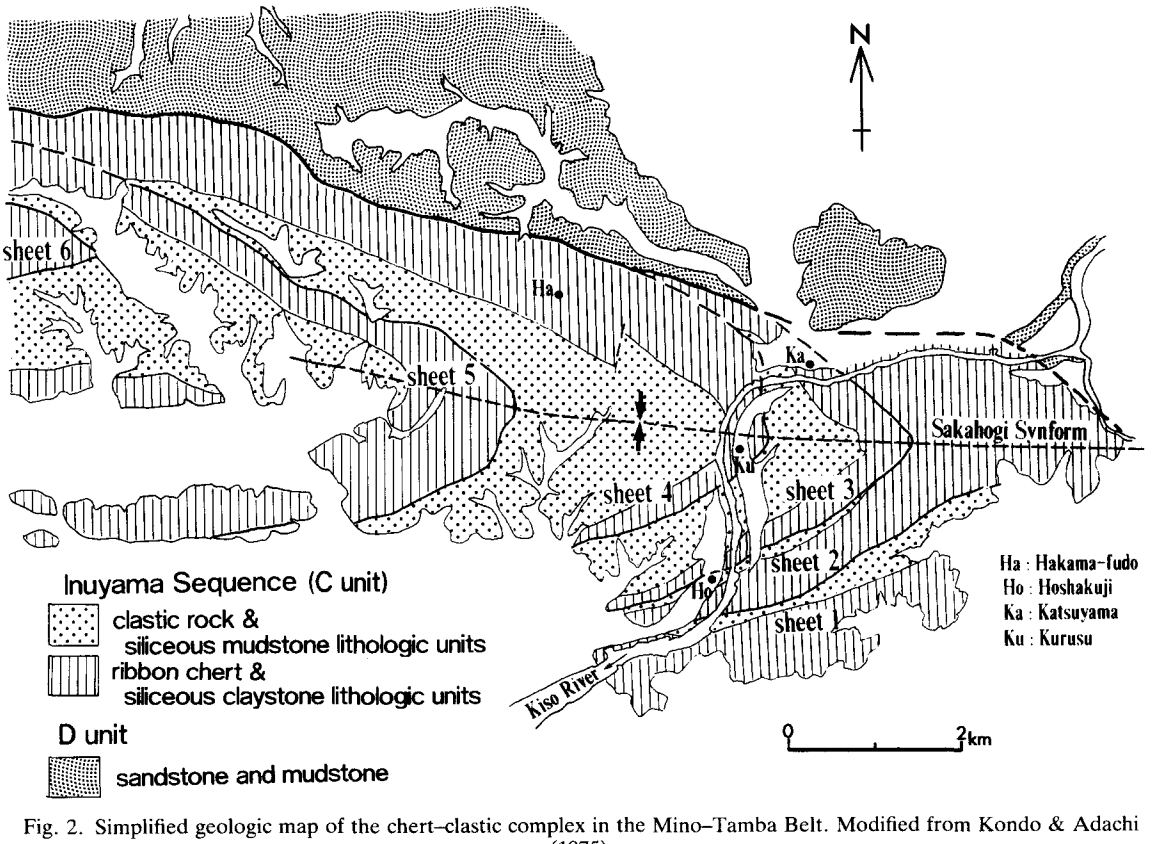

Fig. 2. Simplified geologic map of the chert–clastic complex in the Mino–Tamba Belt. Modified from Kondo & Adachi (1975).

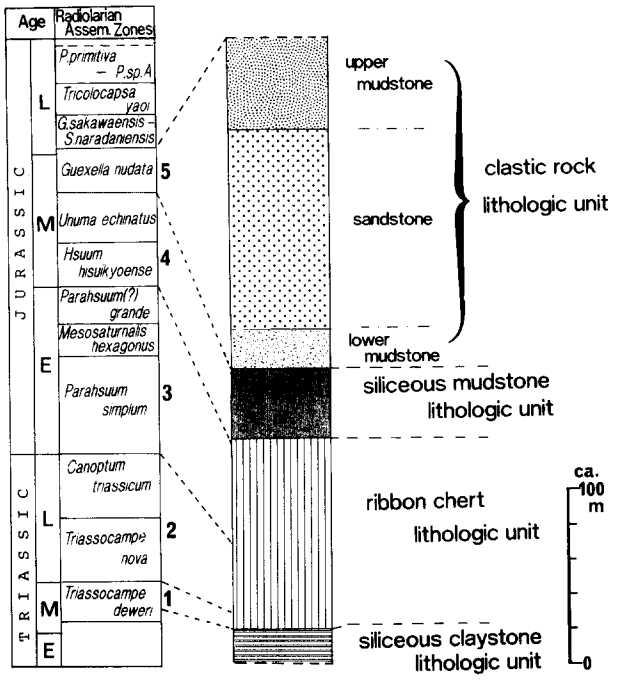

Fig. 3. Stratigraphic column of the Inuyama Sequence and radiolarian assemblage zones. Radiolarian assemblage zones are after Yao *et al.* (1980) and Hori (1990). Numbers 1–5 mark easily established radiolarian assemblages.

structed succession ranges in age from Early Triassic to Middle Jurassic (Fig. 3) (Yao *et al.* 1980, Matsuda & Isozaki 1991). Six regional-scale thrust sheets (referred to as Sheets 1–6 in structurally ascending order in Fig. 2) have been recognized in the Inuyama Sequence and these sheets have been thrust over younger unit D to the south. Unit D consists mainly of turbidite sandstone with intercalated chert and shale, and it yields Late Jurassic radiolarian fossils (Adachi 1988, Otsuka 1988). The Inuyama Sequence in the study area forms a W-plunging synform with a WNW trend (Fig. 2). This was called the Sakahogi synform by Mizutani (1964).

The deformational history of the Inuyama Sequence can be divided into two stages, both of which pre-date Late Cretaceous acidic volcanic rocks. Stage 1 represents accretion-related deformation and it was characterized by progressive deformation, including in-sequence thrusts, out-of-sequence thrusts and F_1 folds. These structures are interpreted to have been generated in a kinematic regime dominated by subhorizontal shortening and (upper over lower plate) S-directed shear. The accretion-related deformation developed during subduction of the Izanagi plate beneath the Asian plate (Maruyama *et al.* 1989). Stage 2 represents intraprism deformation and it was characterized by the development of W-plunging upright folds with wavelengths of 4–12 km (e.g. Matsushita 1953, Sakaguchi 1961, Mizutani 1964). Upright folds such as the Sakahogi synform are arranged in a left-stepping mode against the Median Tectonic Line (MTL), which bounds the southern margin of the Jurassic accretionary complexes (Fig. 1). They formed simultaneously with left-lateral movement along the MTL during the Cretaceous (Hara *et al.* 1977). They are therefore interpreted to have formed in response to left-lateral strike-slip faulting (Hara *et al.* 1977, Otsuka 1991). The Cretaceous strike-slip movement developed in association with the oblique subduction of the Kula-Pacific plate beneath the Asian plate (Taira *et al.* 1983).

Stratigraphic succession

The stratigraphic succession of the Inuyama Sequence is a key indicator for identifying numerous internal detachments and thrust faults as well as for elucidating the depositional environment. It ranges in thickness from 600 to 1000 m, and is grouped into the following four lithologic units, in ascending order (Fig. 3): (1) siliceous claystone; (2) ribbon chert; (3) siliceous mudstone; and (4) clastic rocks. The boundaries of each successive lithologic unit are gradational and fossil ages, including both radiolarian and conodont fossils, indicate consistent younging upward (e.g. Yao *et al.* 1980, Matsuda & Isozaki 1991). The lithologic units therefore make a clear stratigraphic section, although there are numerous detachment zones within the section. This stratigraphic section indicates a transition from pelagite through hemipelagite to terrigenous rocks, including turbidite sandstone and mudstone, thereby reflecting migration of the depocenter from the abyssal plain to the trench floor (e.g. Matsuoka 1984, Lash 1985, Taira *et al.* 1989, Matsuda & Isozaki 1991).

The lowest lithologic unit consists mainly of banded siliceous claystone intercalated with dolomite. The siliceous claystone is greenish gray to black in color, and each band ranges from 2 to 10 cm in thickness. The overlying ribbon chert lithologic unit consists of a rhythmically interbedded sequence of radiolarian chert (with layers 1–10 cm thick) and fine-grained mudstone (layers less than 2 cm thick), which are red and commonly purple, greenish gray or gray in color. The siliceous mudstone lithologic unit is composed of a greenish gray or red terrigenous pelitic rock containing abundant radiolarian fossils, with acidic tuff interbeds in the upper part. The uppermost lithologic unit consists of thick-bedded sandstone, alternating sandstone and mudstone, acidic tuff, and laminated mudstone. With the exception of the acidic tuff, these deposits are similar to "turbidite and its associated clastic rock sequence" described by Mutti & Ricci Lucci (1972). The turbidite origin is suggested by sedimentary structures such as graded bedding, laminations and current marks. This lithologic unit is further subdivided into three subunits: (1) a lower mudstone subunit consisting of laminated mudstone and thin-bedded sandstone; (2) a sandstone subunit composed of thick-bedded sandstone and alternating sandstone and mudstone; and (3) an upper mudstone subunit consisting of laminated mudstone with intercalated acidic tuff and alternating sandstone and mudstone. In addition, a number of sandstone dikes and sills occur in the lower mudstone subunit as well as near the boundary between the chert and siliceous mudstone lithologic units.

Tectonic packets within major thrust sheets

The regional-scale thrust sheets that constitute unit C are cut into slices by numerous internal detachment zones and thrust faults. These outcrop-scale fault zones divide the thrust sheets into many tectonic packets that range in size from meters to up to 500 m. The internal divisions and deformation of these regional-scale thrust sheets are shown schematically in Fig. 4. The tectonic packets are classified into two different types: slices and subslices (Fig. 4). A slice is recognized by a large structural repetition or omission of strata across its boundaries. In contrast, a subslice shows only a difference in structural style of F_1 folds.

In addition to being divisible into tectonic packets, each regional-scale thrust sheet can be divided into lower and upper sheets based on differences in structural style and the presence of a detachment zone within the siliceous mudstone interval (called the 'intrasheet detachment zone') (Fig. 4). The upper sheet consists of the upper stratigraphic section, while the lower sheet consists of the lower stratigraphic section. The lower sheet also displays abundant F_1 mesoscopic folds, while the upper sheet displays very few folds. In addition, fault-related repetitions of strata are more frequently recognized in the lower sheet than in the upper sheet. The multiple repetitions in the lower sheet occur without including rocks of the upper stratigraphic section. The fold–thrust system in the lower sheet, therefore, appears to represent a duplex with the intrasheet detachment zone as a roof thrust, and the basal detachment as a floor thrust.

Geometric relationship between the Sakahogi synform and imbricate structures

The geometric relationship between the Sakahogi synform and the imbricate structures (Fig. 5) is estimated using the geometric method of Ramsay (1967, pp. 491–496), as follows. (1) The method assumes a layer of material bounded by two initially parallel-plane surfaces (surface A in Fig. 5) that remain parallel after folding. The layer contains internal bedding planes (surface B in Fig. 5) inclined to surface A. In the present case, the imbricate structures correspond to surface B, and surface A is an ideal surface forming the synform, approximately corresponding to the boundary thrust of the Inuyama Sequence. (2) The synform axis is calculated from the pi poles to bedding (Fig. 6). The attitudes of strata were measured in homoclinal packets where F_1 folds are missing or rarely developed. The resulting pi axis has a plunge of 78°NW and a trend of N82°W (Figs. 5 and 6). (3) The intersection between the inferred surface A and bedding is nearly parallel to the synform axis (Fig. 5), because the poles of bedding trace out a great-circle.

In order to determine the initial directions of

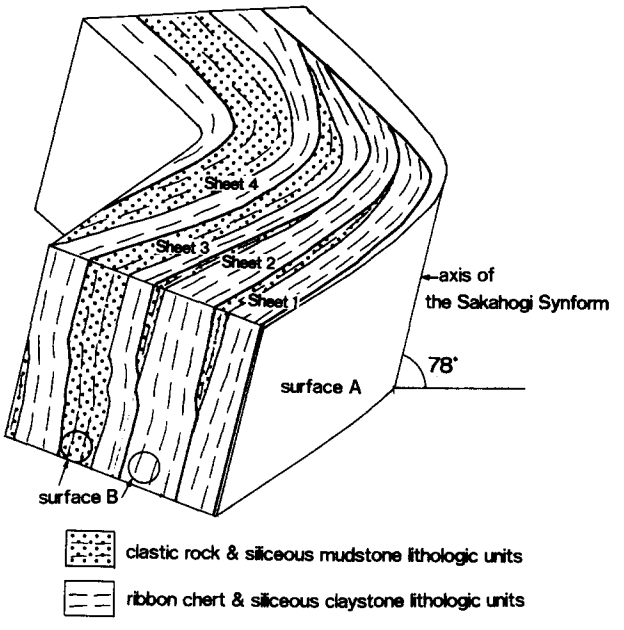

Fig. 5. Relationship between the Sakahogi synform and imbricate structure. Surface A is drawn as a supposed plane forming an ideal cylindrical fold. Surface B is represented as bedding planes.

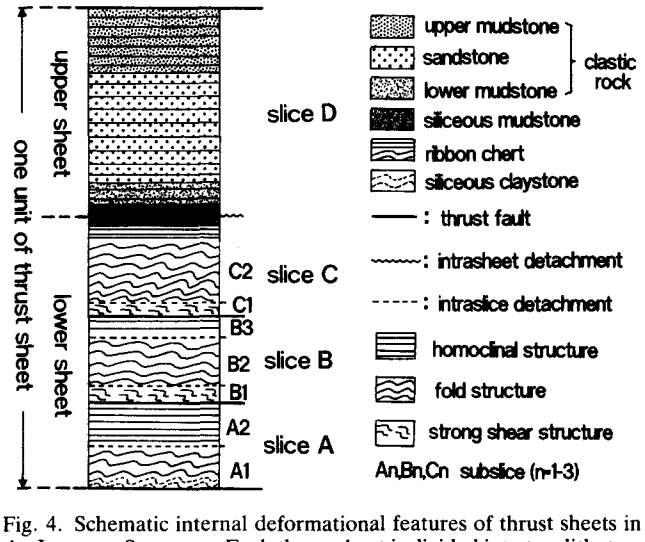

Fig. 4. Schematic internal deformational features of thrust sheets in the Inuyama Sequence. Each thrust sheet is divided into two lithotectonic units based on difference in structural style. These units are subdivided into many tectonic packets, which include slices and subslices. Slices are recognized by large structural repetitions or omission of strata, whereas subslices show only difference in structural style of F_1 folds.

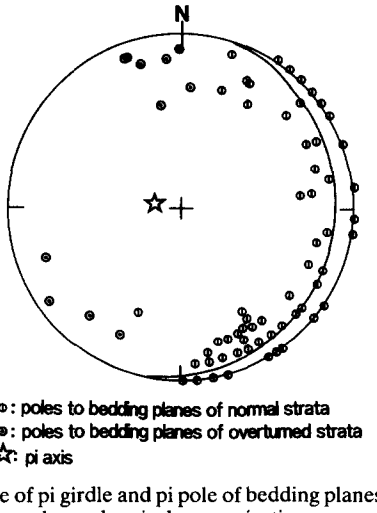

Fig. 6. Attitude of pi girdle and pi pole of bedding planes. Equal-area lower-hemisphere projection.

accretion-related structures in a horizontal bedding reference frame, the effects of the Sakahogi synform have to be considered. Otsuka (1989) adopted the following procedure for unfolding the effects of the synform. First, the northern limb is rotated relative to the southern limb around the synform axis, then bedding is rotated about the regional strike until the beds are horizontal. The observed geometric relationship between the synform and the imbricate structures is consistent with this procedure. In addition, the procedure is consistent with the kinematic interpretation of the synform, as follows. Upright folds such as the Sakahogi synform are interpreted to have formed during Cretaceous time in association with left-lateral movement along the Median Tectonic Line (Fig. 1) (Hara *et al.* 1977, Otsuka 1991). If this is the case the regional-scale N-dipping attitude of strata within the Mino–Tamba Belt is independent of the upright folds. Accordingly, the attitudes of the upright fold axes depend on the attitude of strata resulting from accretion-related tilting. Consequently, we use the same procedure as Otsuka (1989) for unfolding the synform, except for the following modification; both the northern and southern limbs need to be rotated about the synform axis so that they are parallel to the N60°E regional strike of the Inuyama Sequence (Fig. 1). This is because the southern limb is not parallel to the regional strike, but forms an arc (Figs. 2 and 7). Local dip at each locality is calculated using the average strike at the locality and taking the pole to bedding to lie on the pi girdle of Fig. 6.

GEOLOGY ALONG THE COURSE OF THE KISO RIVER

The geologic map along the course of the Kiso River (Fig. 7) extends from the south limb of the Sakahogi synform through the hinge region and into the north limb. It is based on detailed mapping (1:25,000) and biostratigraphic data of the authors and also on the map of Yao *et al.* (1980). Bedding on the south limb of the synform generally strikes ENE–WSW and dips steeply north. In the north limb, bedding strikes NW–SE and dips 70–90° to the southwest.

Yao *et al.* (1980) first reported detailed microfossil studies and presented a simplified geologic map with divisions of regional-scale thrust sheets along this section. Several additional biostratigraphic studies have been carried out on the section (Matsuda *et al.* 1981, Mizutani & Koike 1982, Hori 1986, 1988, 1990, Matsuda & Isozaki 1991). The biostratigraphic data include about 240 microfossil ages that are available to identify tectonic packets. In the case of some chert-dominant slices, such as slice 2B at Hoshakuji and slice 3A at Katsuyama in Fig. 7, microfossil ages have been determined at intervals of from 30 cm to nearly 5 m (Yao *et al.* 1980, Hori 1988).

In this study, in order to clarify the stratigraphic and tectonic division of the section, we have used biostratigraphic data from the above-cited papers and have determined supplementary radiolarian ages (including more than 30 samples from the chert interval and five samples from the clastic rock interval). The new age determinations were carried out at intervals of 1–30 m in chert sections of slice 2C at Hoshakuji and slices 4D and 4F at Kurusu (Fig. 7).

Younging directions within each slice were determined by sedimentary structures in the clastic rocks, radiolarian-based age successions in the ribbon chert, and stratigraphic relations between different lithologic units. Vergence directions for asymmetric F_1 folds were determined after unfolding the Sakahogi synform.

INTERNAL DEFORMATION STRUCTURES OF FAULT SLICES

Fault slices and subslices in the lower sheet of each regional-scale thrust sheet are generally marked by zones of shear deformation at their bases, and F_1 folds increase in both abundance and tightness from top to bottom within each slice (Fig. 4). In contrast, the upper sheet is characterized by homoclinal structures with few mesoscopic F_1 folds (Fig. 4). Typical profile sections of slices in the lower sheet are now described.

Figure 8 is a NNE-trending profile normal to F_1 fold axes across slices 2B and 2C of Sheet 2 at Hoshakuji (Fig. 7). F_1 folds in the profile are gently plunging. Both slices are bounded by N-dipping thrust faults, and are subdivided into several subslices. Three types of subslice have been identified. They are strong shear-type, fold-type and homoclinal-type, on the basis of deformation style. The strong shear-type subslices are characterized by the development of pinch-and-swell structures, tight folds with short wavelengths and layer-parallel faults (e.g. subslices 2B1 and 2C1 in Fig. 8). The fold-type subslices contain abundant mesoscopic F_1 folds (e.g. subslices 2B2, 2C2 and 2C3 in Fig. 8). The homoclinal-type subslices contain rare folds or other shear deformational structures (e.g. subslices 2B5 and 2B8 in Fig. 8). In each slice, these subslices are generally arranged in an ascending vertical sequence consisting of the strong shear-, fold- and homoclinal-types (Fig. 8); thin fold-type subslices are sometimes intercalated in the upper part of this sequence. In addition, within the fold-type subslices, F_1 folds tend to decrease upwards in terms of both abundance and tightness.

The horizontal sketch map (Fig. 9) of Sheet 3 at Katsuyama (Fig. 7) shows a typical vertical change in the style of F_1 mesoscopic folds within a slice. The mesoscopic folds plunge steeply in this location. There are three intraslice detachment zones (a,b and c) that influence the style of F_1 folds within the ribbon chert (Fig. 9). F_1 folds begin to form just above the sole thrust of Sheet 3 to the east of Fig. 9 and gradually disappear upward in the area of Fig. 9.

The lower sheet of Sheet 4 includes megascopic isoclinal recumbent folds. Right-side-up slices alternate with overturned slices at intervals of 50–150 m (Fig. 7). The presence of overturned strata reveals that mega-

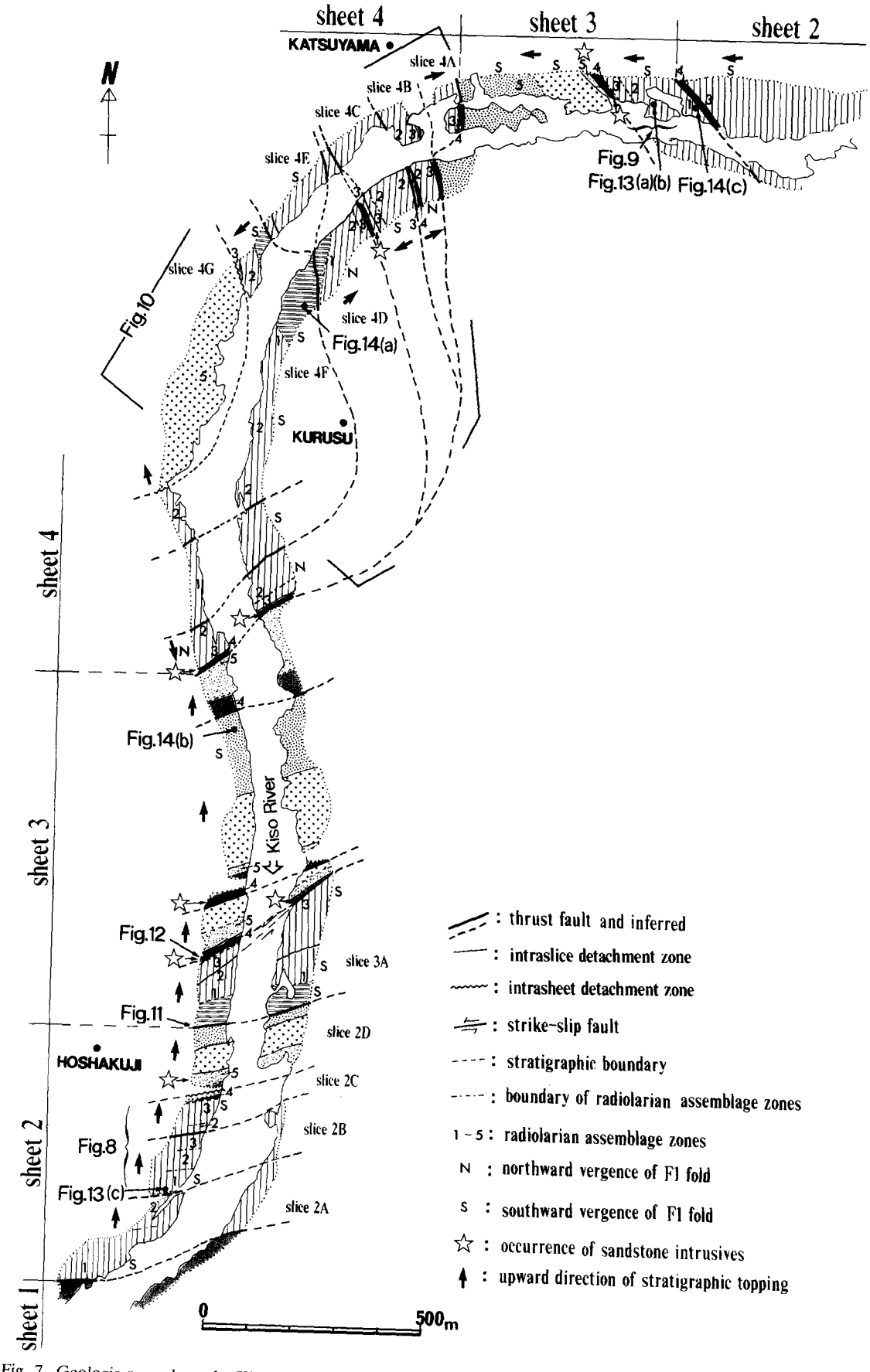

Fig. 7. Geologic map along the Kiso River from Hoshakuji to Katsuyama (see Fig. 2 for location). The legend for the lithologic units and radiolarian assemblage zones is given in Fig. 3. Some of the radiolarian assemblages were described during this study, and they are augmented by data from Yao *et al.* (1980) and others.

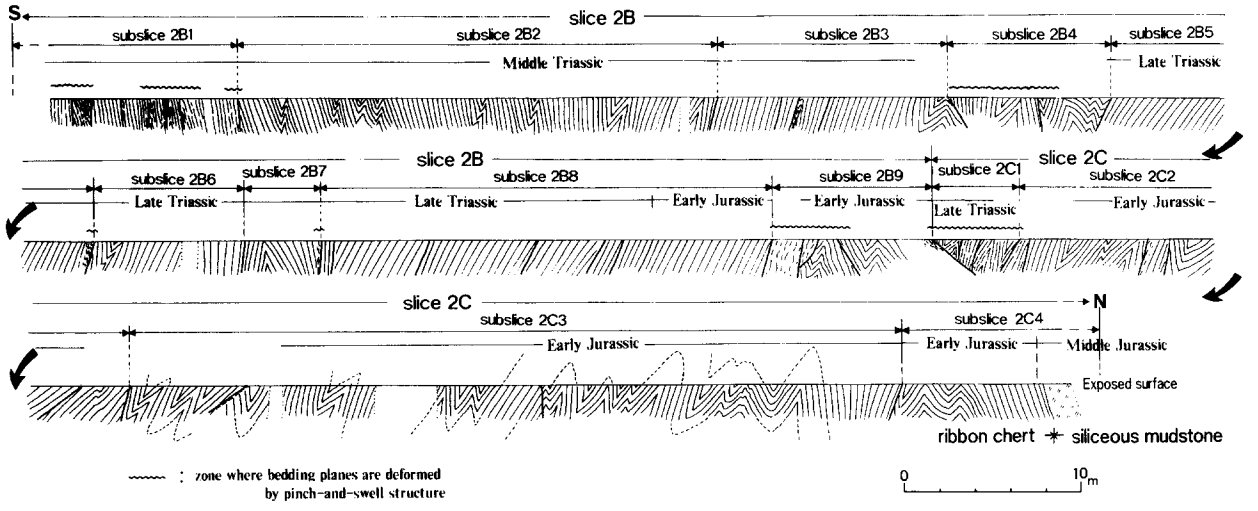

Fig. 8. Detailed cross-section of Sheet 2 along the west bank of the Kiso River at Hoshakuji, showing the internal subdivision of slices and subslices in the ribbon chert. The ages of each subslice are after Yao *et al.* (1980), Matsuda & Isozaki (1991) and our present study. Striped pattern indicates ribbon chert and dotted pattern siliceous mudstone.

scopic isoclinal folds with wavelengths of 100–300 m formed in Sheet 4. The axial planes of these folds are cut by thrust faults (Fig. 7). Vergence directions of F_1 folds within slices change according to the younging directions of bedding in the slices; S-verging F_1 folds occur in slices with right-side-up bedding, whereas N-verging folds occur in slices with overturned bedding (Fig. 7). Therefore, the isoclinal folding in Sheet 4 was accompanied by parasitic F_1 mesoscopic folding on the limbs. These structural features are illustrated in cross-section in Fig. 10, which is constructed from the map view between the north limb and the hinge region of the Sakahogi synform (Fig. 7), where F_1 fold axes plunge steeply.

In summary, with the exception of overturned-bedding slices, the internal deformation of individual slices in the lower sheet is characterized by intense shearing at the base and an upward decrease in the intensity of folding, as schematically illustrated in Fig. 4. The geometrically close relationship between folds and

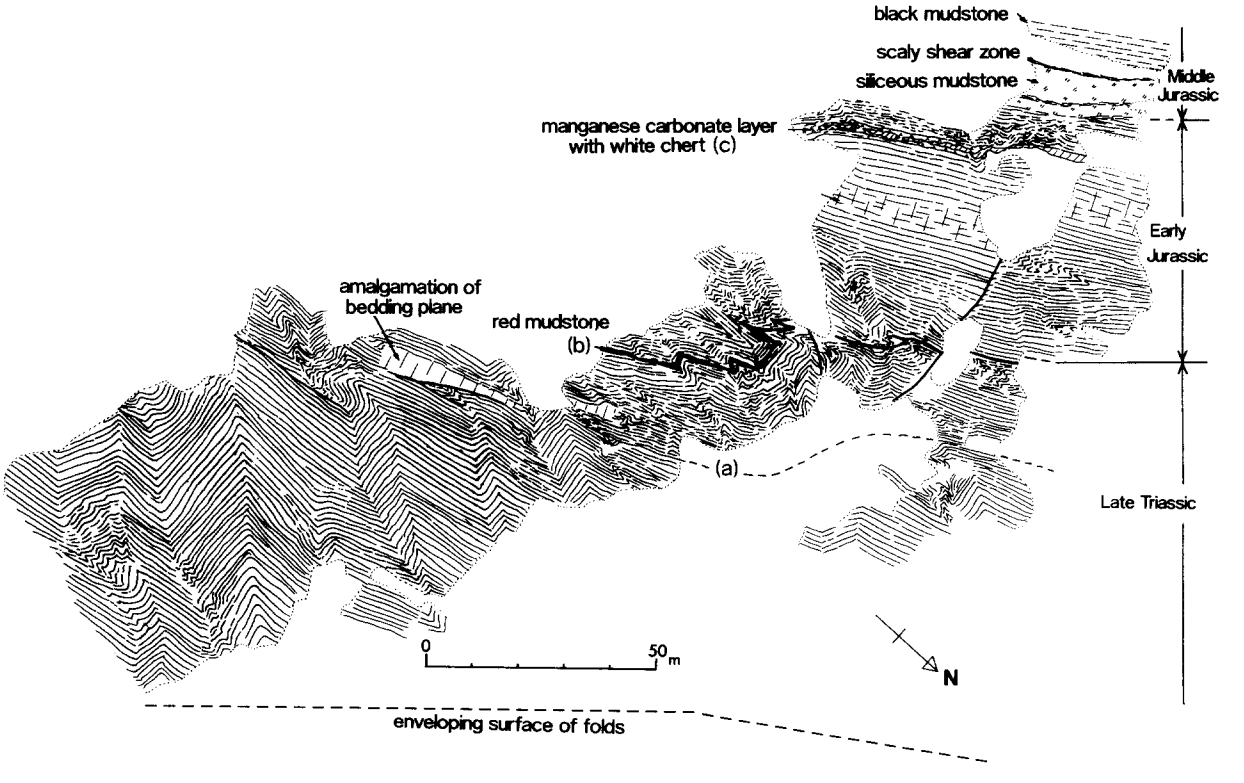

Fig. 9. Horizontal sketch map of the ribbon chert in Sheet 3 exposed on the north side of the Kiso River at Katsuyama (see Fig. 4 for location). (a), (b) and (c) indicate intraslice detachment zones (see text for explanation). The enveloping surfaces of folds are subparallel to the general attitude of Sheet 4. The ages of the ribbon chert are after Hori (1990) and our present study.

thrust faults suggests that F_1 folds developed in a shearing regime associated with thrusting at the base of slices and thrust sheets.

THRUST FAULTS AND DETACHMENT ZONES

Numerous internal detachment zones or thrust faults have also been recognized along the strip map of Fig. 7. These faults are generally layer-parallel, but they locally cross bedding at small angles (e.g. Figs. 8 and 9). The presence of these faults is identified by juxtaposed packets of different lithology, internal structural fabric, or age, as well as by slickensided surfaces and scaly clay fabric.

Thrust faults which produce structural repetitions of strata are commonly associated with conspicuous shear zones and other indicators of deformation. Among these, sole thrusts at the bases of thrust sheets (Fig. 7) are secondary thrust faults that overprint the initial thrust fault systems, because sole thrusts truncate the intrasheet detachments separating the upper sheets and the lower sheets, and truncate the internal structures of thrust sheets at ramps as shown in the northern limb of the Sakahogi synform in Fig. 2. Secondary imbricate thrusting is interpreted as out-of-sequence thrusting. Broad scaly fabric zones with a well-developed scaly foliation, spaced from 50 to 120 cm, are particularly well developed in association with sole thrusts. The shear zones are composed of scaly siliceous mudstone and include lenses of chert and sandstone (Fig. 11). Scaly foliation surfaces in mudstone are polished and striated, indicating that they are slip surfaces. The absence of the lithologies found in the shear zones (including siliceous mudstones and cherts) in the nearby hanging-walls and footwalls suggests that these distinctive lithologies were derived from an interval of equivalent lithology at lower structural levels and carried into the shear zone during thrusting. The subsidiary structures locally associated with these sole thrusts include small-scale duplexes, asymmetric boudinage due to Riedel shearing, and drag-fold structures. These structures provide information about the direction of propagation along the sole thrusts. In the hanging-wall of the sole thrust of Sheet 3 at Katsuyama (Figs. 7 and 14c), for example, the geometric features of two small duplexes indicate the same southward transport direction (in a horizontal-bedding reference frame) as the vergence of F_1 folds observed in the same area.

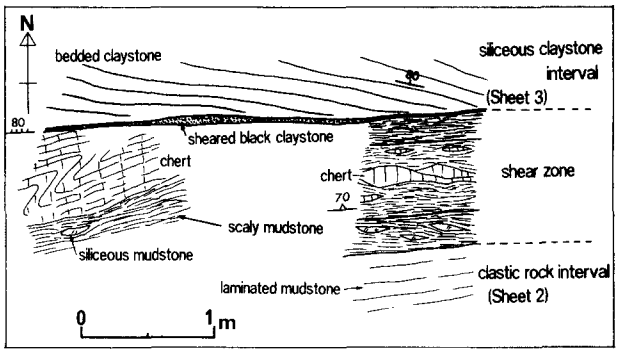

Fig. 11. Sketch of scaly shear zone forming the sole thrust of Sheet 3 at Hoshakuji (see Fig. 7 for location). All the scaly mudstone in the shear zone can be interpreted to have been derived from the siliceous mudstone interval, based on lithologic similarity.

Intrasheet detachment zones within the siliceous mudstone intervals are structurally significant fault zones that separate two lithotectonic parts of each thrust sheet (Fig. 4). These broad zones of scaly fabric range in width from 50 to 200 cm (Fig. 12). Other minor detachment zones are common along boundaries between stiff and soft lithologies. Most of the boundaries between the sandstone and the mudstone subunits of the clastic rock interval are marked by cataclastic fault surfaces parallel to bedding (Fig. 7). In the ribbon chert unit, interbedded

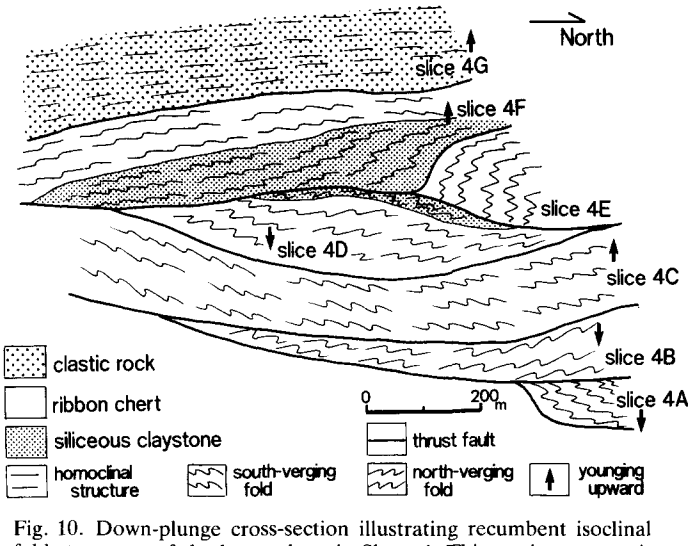

Fig. 10. Down-plunge cross-section illustrating recumbent isoclinal fold structures of the lower sheet in Sheet 4. This section, approximately normal to F_1 fold axes, is constructed from the map view of the region from the north limb to the hinge of the Sakahogi synform after unfolding the synform (Fig. 7). Bedding structures within slices are presented schematically (see Fig. 7 for location).

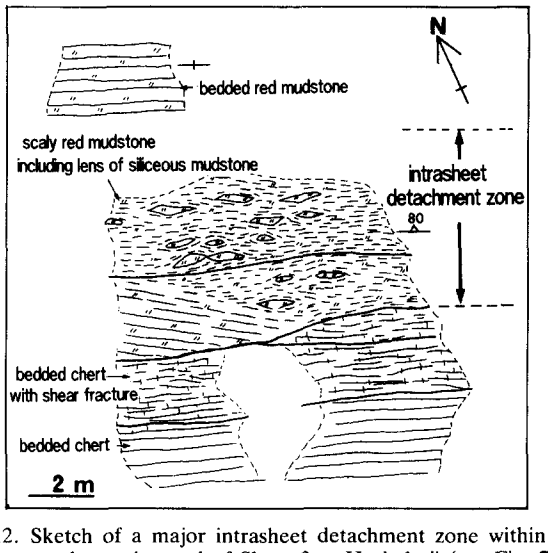

Fig. 12. Sketch of a major intrasheet detachment zone within the siliceous mudstone interval of Sheet 3 at Hoshakuji (see Fig. 7 for location).

mudstone layers commonly behaved as internal detachment zones (e.g. zones a and b in Fig. 9). In the lowest siliceous claystone, detachment zones tend to develop along interbeds of black carbonaceous claystone.

F_1 FOLDS

F_1 folds developed primarily in the ribbon chert and siliceous claystone intervals, but a few can be observed in the clastic rock intervals. They are classified into mesoscopic (half-wavelengths ranging from 20 to 500 cm), and megascopic (half-wavelengths ranging from 10 to 150 m) folds.

Style of mesoscopic F_1 *folds*

The shapes of mesoscopic F_1 folds are controlled by lithology.

Chert. F_1 folds in the chert intervals commonly have interlimb angles ranging from 30° to 120° (Figs. 9 and 13), although folds with smaller interlimb angles (10–30°) are found in the strong-shear type subslices (Fig. 13c). Most of the folds have asymmetric chevron fold geometries with sharp hinge zones and planar or slightly undulating limbs (Figs. 9 and 13a). Some exhibit conjugate and concentric fold geometries. Hinge lines tend to undulate. Fold limbs are slightly deformed by pinch-and-swell structures associated with layer-parallel extension during folding (Fig.13b); slickensided bedding with striations is also common. Chert layers are generally 1.1–1.9 times thicker in the hinges than in the limbs of folds (Fig. 13b). Flexural flow in interbedded mud layers between competent chert layers produced more thickening in the hinge regions (Fig. 13b). In addition, disharmonic folds occur either side of a relatively thicker red mudstone layer (mudstone b in Fig. 9, ranging from 5 to 10 cm thick); the chert layers beneath it are folded into broad anticlines and synclines, whereas the chert layers above it are folded into tight anticlines and synclines.

Hinge areas are commonly fractured and contain contractional shear fractures, normal shear fractures, dilational fractures, axial-plane cleavage and bedding-parallel stylolites. With the exception of stylolites, these structures are closely related to flexure-slip folding and flattening normal to the axial surfaces. The stylolites evidently developed during loading in an earlier diagenetic stage, because they are bedding-parallel and cut by the other fractures, as Brueckner & Snyder (1985) also noted in similar lithologies in the United States. Microscopic observation of thin sections from hinge areas of these folds reveals the following features. Tests of radiolaria and sponge spicules are usually arranged parallel to bedding, whereas they are partly rearranged parallel to axial planes in mudstone layers. Tests of radiolaria are usually undeformed, although they are elongate slightly parallel to axial surfaces near the fold hinges where axial-plane cleavages are best developed.

Siliceous claystone. F_1 folds, with half-wavelengths ranging from 10 to 50 cm, are usually close with interlimb angles of 20–40° (Fig. 14a). Claystone layers are generally 1.5–2 times thicker in the hinges than in the limbs of folds. Black claystone layers are relatively incompetent and locally injected into light-colored competent layers parallel to the axial surface (Fig. 14a). Dolomite interbeds behaved competently during folding, because they form parallel-fold geometries.

Clastic rocks. F_1 folds in the clastic rock intervals are found at only four localities. These folds generally have parallel-fold geometries and show slight thickening of the sandstone and mudstone layers in the hinge zones. Interlimb angles are generally 60–120°, and fold half-wavelengths vary from 50 to 600 cm (Fig. 14b).

Attitude of F_1 *folds*

The attitudes of F_1 folds provide information about the transport direction of thrusting, because F_1 folds are considered to have formed in association with thrusting, as mentioned above. The axes and axial planes of F_1 mesoscopic folds in the ribbon chert and the siliceous claystone intervals were measured in each thrust sheet along the section in Fig. 7, and in Sheet 4 along a road-cut exposure at Hakama-fudo in Fig. 2. The results are shown in Fig. 15. Each diagram in the figure shows a fairly good concentration of orientation data. The attitudes of F_1 folds systematically change from the south limb to the north limb of the Sakahogi synform.

The effect of the Sakahogi synform was removed by the procedure described earlier to obtain the initial orientations of F_1 folds in a horizontal-bedding reference frame. The resulting fabric of F_1 mesoscopic folds after restoration (Fig. 16) shows that the average orientation of fold axes is approximately E–W, and the vergence direction is southward. Accordingly, the sense of simple shear during folding was approximately southward, reflecting S-directed overthrusting.

SANDSTONE INTRUSIONS

Many sandstone dikes and sills were intruded prior to thrust sheet emplacement. The intrusions are restricted to the lower mudstone subunit of the clastic rock intervals and near the boundary between the siliceous mudstone and the ribbon chert intervals (Fig. 7). The intrusions in the chert intervals of Sheet 4 have been described by Otsuka (1989).

The dikes and sills are of variable size, shape and attitude. They range from less than 1 to 100 cm in width and from 5 to more than 400 cm in length, and they contain fine- to medium-grained, well-sorted sand. More than 100 individual intrusions were found in the lower mudstone horizon. The dikes there were injected upward or downward, and locally branched from sills. The directions of emplacement of these dikes were determined by the form of branching from sills or the

depositional source layers and also by directions of tapering. Some dikes in the lower mudstone part grade into depositional sandstone beds with sedimentary structures such as graded bedding and cross laminations. In contrast, in the siliceous mudstone and ribbon chert intervals, most intrusions are sills, which have been deformed to form pinch-and-swell structures and lenticular bodies arranged parallel to bedding.

Otsuka (1989) pointed out that, based on mineral compositions, sandstone intrusions within the siliceous mudstone and the ribbon chert intervals originated from sandstone beds of the clastic rock intervals. This conclusion is supported by the presence of downward-injected dikes in the lower mudstone intervals and by the absence of depositional sandstone layers in both the siliceous mudstone and the ribbon chert intervals. As for the clastic rock intervals, the intrusions occur only in the lower mudstone subunit. We conclude, therefore, that they were derived from sand layers intercalated with mudstone in the lower mudstone subunit.

Layer-parallel faults with zones of scaly fabric (ranging in thickness from 1 to 5 cm) are common in the lower mudstone part of the clastic rock interval. The faults cut some sandstone dikes, while they are intruded by others. The sand intrusions, therefore, formed roughly simultaneously with the layer-parallel faulting.

The sandstone intrusions are not due to near-surface slumping, because parallel laminae of surrounding mudstone are not disturbed. Some sandstone sills are folded with chert layers (Otsuka 1989), and it should be noted that the folds discussed by Otsuka (1989) belong to the F_1 fold group described in this paper. In addition, sandstone sills within the siliceous mudstone are commonly affected by shear deformation related to thrusting. Consequently, the sandstone intrusions are interpreted to have been initiated tectonically in association with layer-parallel faulting before the main deformational phase characterized by thrusting and folding.

DISCUSSION

Kinematic development of F_1 *folds in chert*

Several studies of mesoscopic folds in ribbon chert associated with accretionary complexes (Ramberg & Johnson 1976, Miller *et al.* 1982, Wahrhaftig 1984, Brueckner & Snyder 1985, Otsuka 1989) have recognized common features such as asymmetric chevron fold geometries and fairly well concentrated attitudes of fold axes and axial planes. In addition, Brueckner & Snyder (1985) noted that mesoscopic folds in chert were produced under confining pressures high enough to form layer-parallel microstylolites. These structural features suggest that the mesoscopic folds commonly developed in the chert did not originate as slump folds, but were produced tectonically.

The mesoscopic F_1 folds in the ribbon chert in the Inuyama Sequence are similar to those described elsewhere, and in addition, detailed structural studies demonstrate that F_1 folds in the Inuyama Sequence formed in association with thrust propagation. We may discuss, therefore, the evolution of F_1 folds in the chert in the context of the development of imbricate thrust systems in the Inuyama Sequence.

The transformation from opal-A through opal-CT to quartz results in major changes in physical rock properties of chert (Murata & Larson 1975, Isaacs 1981). Accordingly, mesoscopic features of folds in chert can be used to assess the silica-diagenetic condition during folding (Snyder *et al.* 1983, Brueckner *et al.* 1987). In the Inuyama Sequence, the thickening of both chert and mudstone in the hinges of F_1 folds, and the lack of flattened radiolarian shells indicate that both chert and mudstone were soft enough to permit inter-granular flow during folding, although chert layers were competent enough to produce a chevron geometry by flexural-slip folding. In addition, the development of microstylolites prior to folding suggests that high confining pressures existed in the ribbon chert before folding.

Snyder *et al.* (1983) and Brueckner *et al.* (1987) proposed the deformation–diagenesis model, which links the diagenesis of siliceous sedimentary rocks to the mode of deformation observed in the Miocene Monterey Formation of California. Numerous box, chevron and parallel folds are associated with thrust faults, and they are found only in layers composed of CT-porcelanite and CT-chert. The other, opal-A or quartz, silica diagenetic conditions are not favorable for the formation of such folds. The above deformation-diagenesis model may be applied to the Inuyama Sequence. Accordingly, F_1 folds of the Inuyama Sequence probably formed during the diagenetic stage in which ribbon chert was still interbedded CT-chert and CT-porcelanite. This physical condition appears to facilitate the formation of the fracture systems and intergranular flow associated with folding.

The diagenetic condition during deformation noted above provides a constraint on the temperature. The temperature of the transformation of opal-CT to quartz in the sedimentary realm is interpreted to be within the range of 31–165°C (e.g. Murata & Larson 1975, Mizutani 1977, Williams *et al.* 1985). Accordingly, the maximum temperature at the time the ribbon chert was folded was probably below 165°C.

Evolution of the offscraping accretionary process

The Inuyama Sequence is characterized by stacked thrust sheets composed of oceanic plate stratigraphy. Such a stratigraphic section implies that the depositional site migrated from the abyssal plain to the trench floor (e.g. Matsuoka 1984, Taira *et al.* 1989, Matsuda & Isozaki 1991). We consider, therefore, the structural evolution of the Inuyama Sequence in the context of the accretionary process associated with subduction of an oceanic plate. The Inuyama Sequence was initially deformed at the silica diagenetic condition of opal-CT: at the time, the maximum temperature was below 165°C. In addition, metamorphic studies indicate that melange

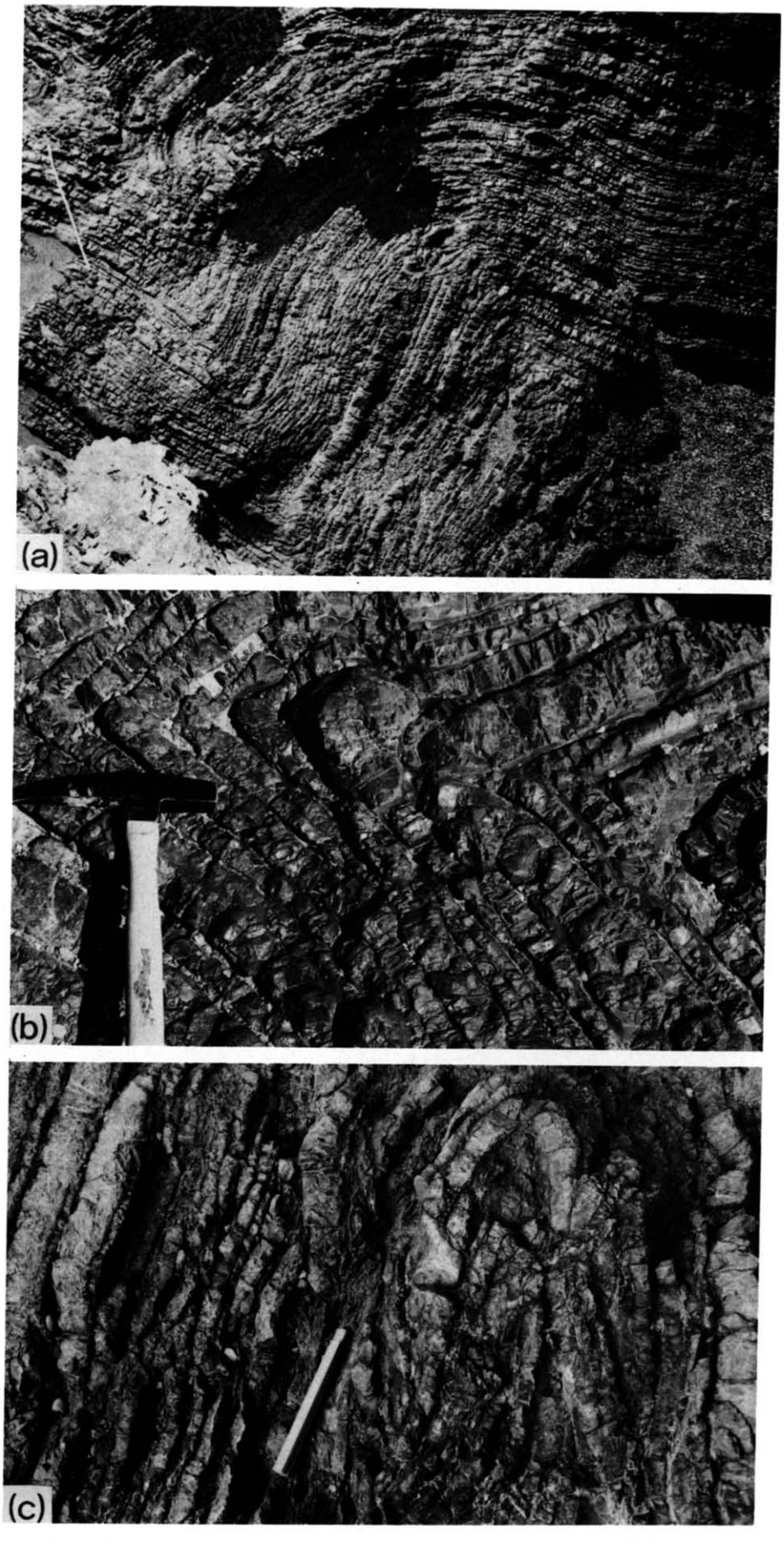

Fig. 13. F_1 folds in ribbon chert. (a) Chevron folds with steeply plunging axes in Sheet 3 at Katsuyama (Fig. 7). Scale bar is 1 m long. (b) Close-up of the hinge of a chevron fold from Sheet 3 at Katsuyama (Fig. 7). Note that the thicknesses of the folded layers, especially the mudstone layers, are greater in the hinge than in the limb. The hammer is 30 cm long. (c) Tight folds deformed by pinch-and-swell structure from subslice 2B1 of Sheet 2 at Hoshakuji (Fig. 7). Scale bar is 20 cm long.

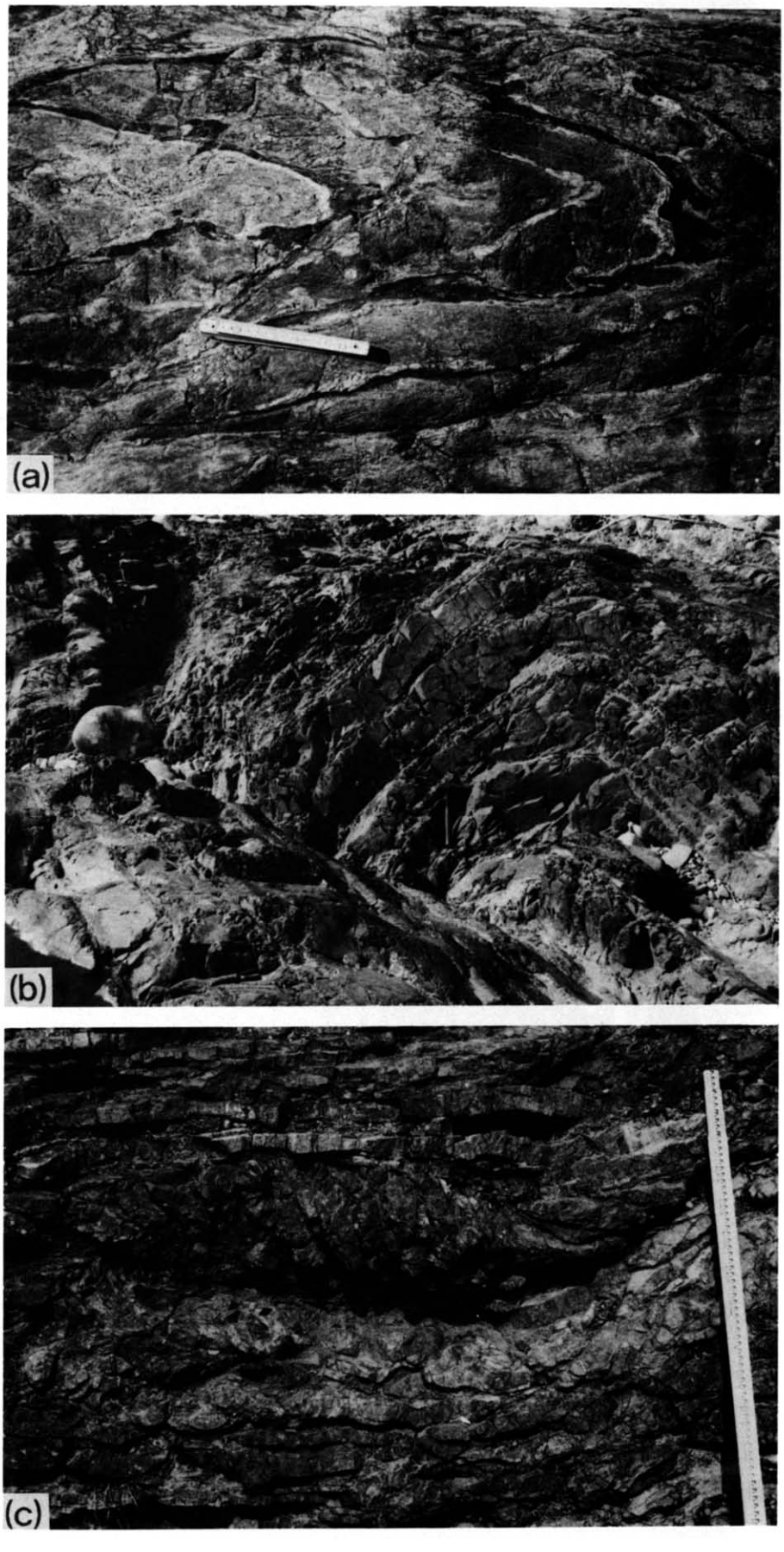

Fig. 14. (a) Tight F_1 fold in the siliceous claystone interval from Sheet 4 at Kurusu (Fig. 7). Note the similar fold geometry. Scale bar is 20 cm long. (b) Open F_1 fold in the clastic rock lithologic unit from Sheet 3 at Kurusu (Fig. 7), showing a concentric fold geometry with southward vergence. The rocks are interbedded acid tuff and tuffaceous shale. The hammer is 30 cm long. (c) Mesoscopic duplex structure developed in ribbon chert from the base of Sheet 3 at Katsuyama (Fig. 7). Scale bar is 120 cm long.

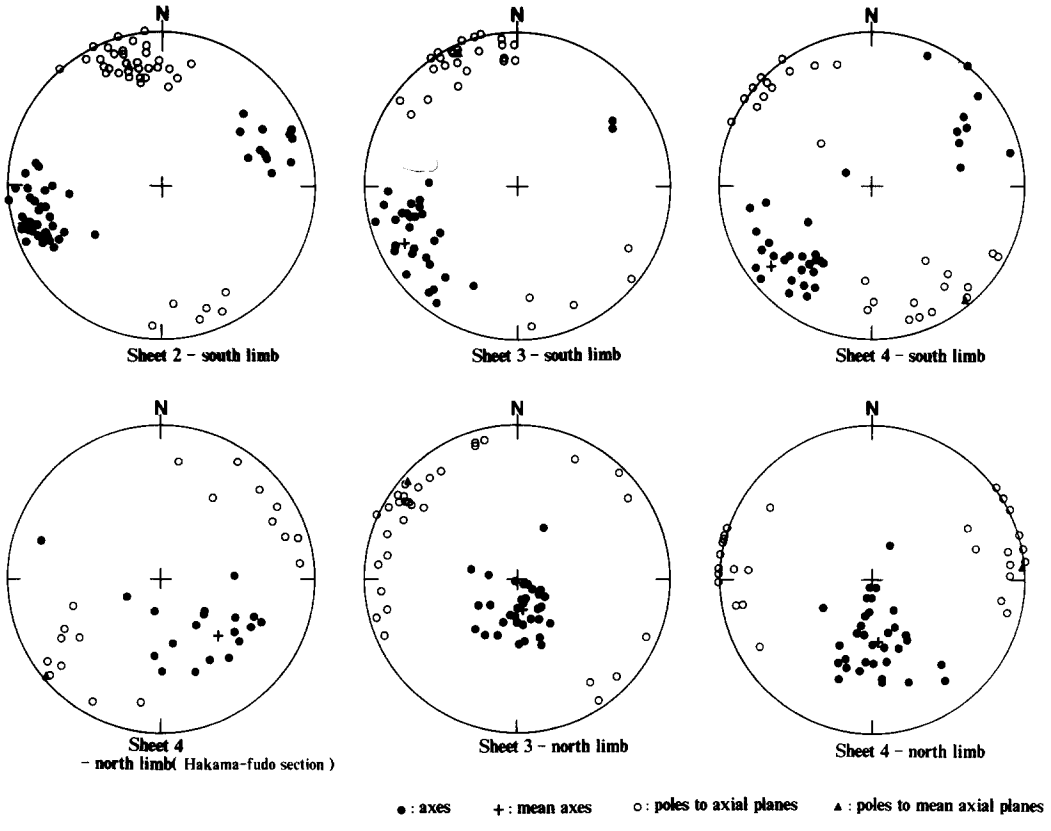

Fig. 15. Attitudes of fold axes and poles to axial planes of mesoscopic F_1 folds in ribbon chert and siliceous claystone at six localities. The Hakama-fudo section (Sheet 4) is located at Hakama-fudo (Fig. 2), and the other localities lie along the section shown in Fig. 7. Equal-area lower-hemisphere plots.

units including basaltic rocks suffered the regional metamorphism of prehnite–pumpellyite to pumpellyite–actinolite facies (Hashimoto & Saito 1970). Thus the Inuyama Sequence, which is characterized by coherent sedimentary rocks without basaltic rocks, is interpreted to have been accreted at shallower structural levels than the melange units that include basaltic rocks. The Inuyama Sequence has probably not been buried below the depth of prehnite–pumpellyite facies metamorphism, as Matsuda & Isozaki (1991) pointed out.

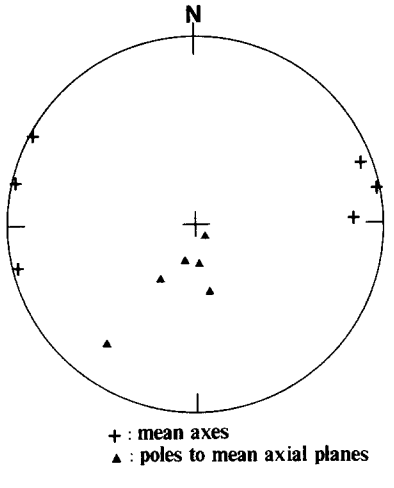

Fig. 16. Attitudes of mean fold axes and mean poles to axial planes of mesoscopic F_1 folds in a horizontal-bedding reference frame. Each data point was located by removing the effect of the Sakahogi synform from the means of measured data shown in Fig. 15. See text for the procedure. Equal-area lower-hemisphere projection.

The profile section of thrust systems parallel to the transport direction provides geometric constraints of the accretionary process. The geometric pattern of southward-stepping imbrication has been recognized in horizontal map view from the north limb to the hinge of the Sakahogi synform (Fig. 2). This section closely parallels the transport direction because F_1 fold axes plunge steeply in this location (Fig. 5). Figure 17 shows the down-plunge cross-section derived from the above section after unfolding of the Sakahogi synform above the sole thrust of the Inuyama Sequence. The sole thrust was rotated to be horizontal. The dips of bedding in the thrust sheets (Fig. 17) approximately reflect their strikes in the map view of Fig. 2. The transport direction of thrust sheets is southward, based on the attitude of F_1 folds (Fig. 16). Accordingly, this section shows a S-verging imbricate system, in which each thrust sheet converges downward to the sole thrust of the Inuyama Sequence.

The geometric pattern of imbricate thrusts (Fig. 17) appears to resemble that found near the frontal part of submerged modern accretionary prisms studied by Seely *et al.* (1974), Westbook *et al.* (1984), Moore *et al.* (1990) and many others. The structural evolution of the Inuyama Sequence, however, is not consistent with relatively simple accretionary models of sequential off-scraping (Otsuka 1989) or underthrusting (Matsuda & Isozaki 1991). The main reasons are that each thrust sheet is (1) subdivided into two distinct lithotectonic units—an upper sheet and a lower sheet representing a

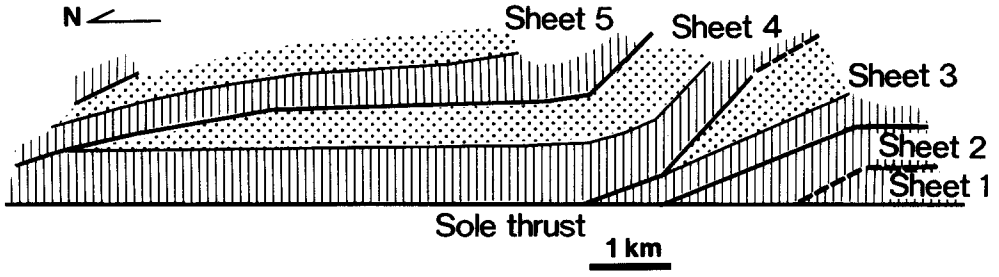

Fig. 17. Southward-verging imbricate structure of the Inuyama Sequence derived from the map view from the northern limb to the hinge of the Sakahogi synform in Fig. 2, after unfolding the synform. The bedding dips in the thrust sheets were drawn based on the strikes shown on the map of Fig. 2. See text for explanation. The legend for the lithologic units is shown in Fig. 2.

duplex structure, and (2) bounded by a sole thrust regarded as an out-of-sequence thrust.

On the basis of the above structural and stratigraphic features, we present a tectonic model for the offscraping accretionary process in the Inuyama Sequence (Fig. 18). In this model, in-sequence thrusts have a lateral spacing of approximately 3.5 km and a dip of 17°; in contrast out-of-sequence thrusts have a lateral spacing of 1.5 km and a dip of 10° so that the resulting geometry (refer to rectangle A in Fig. 18) may be comparable to that of the exposed regional-scale imbricate thrust system of the Inuyama Sequence shown in Fig. 17. This model demonstrates the structural evolution in the frontal 20 km of the prism. It is characterized by in-sequence thrusting, down-stepping of the décollement and out-of-sequence thrusting. Initial in-sequence thrusting within the lower and the upper sheets (imbricate thrust zone) was overprinted by secondary prism thickening in the form of out-of-sequence thrusting.

In our interpretation (Fig. 18) the décollement zone was initiated along the siliceous mudstone horizon (the intrasheet detachment), and then it stepped down-section into the lowest siliceous claystone horizon at deeper structural levels. The combined thickness of the ribbon chert and the siliceous claystone intervals suggests that this step of the décollement is 100–150 m high. The intrasheet detachment zone within the siliceous mudstone interval is characterized both by the stratigraphic control of its position and by the associated broad zone of scaly fabric (Fig. 7). In these features it is comparable to basal décollement zones in the frontal areas of modern accretionary wedges (Moore *et al.* 1986, Moore 1989). We regard therefore the intrasheet detachment zone as the fossil initial décollement zone. The propagation of the décollement zone seaward of the deformation front is also supported by the generation of layer-parallel faulting and high pore pressure just above the décollement horizon before folding and thrusting. This caused the sandstone intrusions. Changes in level of this décollement may be due to the formation of duplex structures within the lower sheet below the initial décollement zone; these duplexes appear to have been caused by the collapse of the footwall of the décollement.

The position of the décollement is consistently restricted to two stratigraphic levels: the siliceous mudstone interval and the siliceous claystone interval. Presumably, at the time of accretion, the ribbon chert, which was composed of interbedded CT-chert and CT-porcelanite, was much more competent than both the siliceous mudstone and the siliceous claystone. In addition, the low permeability of the chert and muddy rocks would have tended to cause high pore pressure in the lower stratigraphic section, particularly when these rocks become tectonically compacted. High pore pressure leads to lower shear strength. Recent studies of modern accretionary prisms offer analogs of the development of a décollement at a horizon of less-permeable and incompetent rocks such as intervals of hemipelagic mud (e.g. Moore 1989).

The sandstone intrusions in the Inuyama Sequence were injected downward from the lower mudstone to the boundary between the chert and the siliceous mudstone intervals prior to folding and thrusting. The vertical distance of injection is estimated to be over 30 m, based on the typical thickness of the siliceous mudstone intervals. At the time of intrusion, some physical or structural conditions were probably generated so that the potential energy of intrusion overcame the lithostatic pressure and buoyancy. Causes of downward clastic injection have been proposed as follows: (1) the development of extensional faults as conduits (e.g. Harm 1965); (2) the generation of fluid pressure equal to lithostatic pressure (DiTullio & Byrne 1990). It is likely that these conditions also existed in the case of the Inuyama Sequence. As for (1), in modern convergent margins, the sediment cover is usually cut through to the seafloor by steeply-dipping normal faults that step blocks down towards the trench (e.g. Hilde 1983, Aubouin *et al.* 1984, Brown & Behrmann 1990), although such regional-scale normal faults have not been found in the study area. As regards (2), the lithological condition at the stratigraphic horizon at which sandstone intrusions occurred makes it a likely site for the generation of high fluid pressure. Consequently, these two conditions probably allowed for the downward-injection of the intrusions.

The development of out-of-sequence thrusting is common in modern accretionary prisms (e.g. Kagami *et al.* 1985, Behrmann *et al.* 1988) and in foreland fold-and-thrust belts (e.g. Coward 1980, Morley 1988), although little is known from ancient accretionary complexes, except for two examples in the Eocene Shimanto Belt in southwest Japan (Nishi 1988, DiTullio & Byrne 1990).

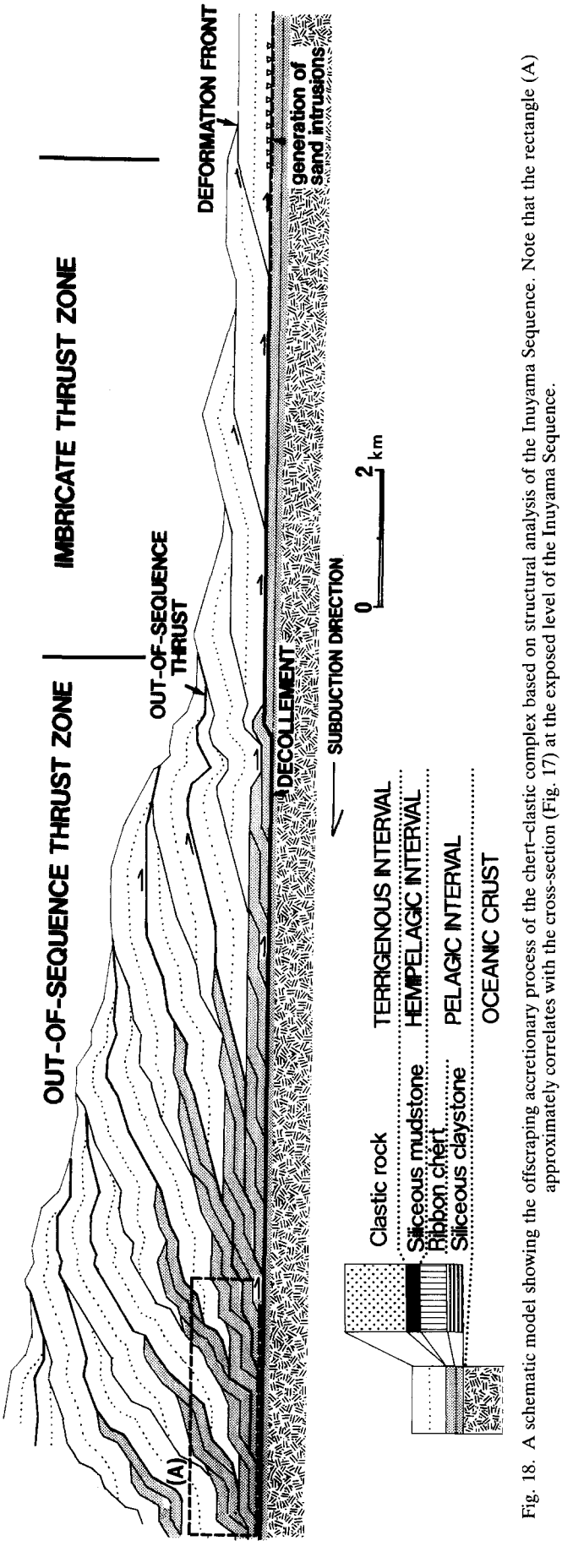

Fig. 18. A schematic model showing the offscraping accretionary process of the chert–clastic complex based on structural analysis of the Inuyama Sequence. Note that the rectangle (A) approximately correlates with the cross-section (Fig. 17) at the exposed level of the Inuyama Sequence.

As for the kinematic significance of out-of-sequence thrusting in modern prisms, Behrmann *et al.* (1988) pointed out that, with limited back-rotation of thrust slices, the formation of out-of-sequence thrusts is geometrically necessary to maintain the critical taper of the accretion wedge. Nishi (1988) first suggested the presence of out-of-sequence thrusts in ancient accreted rocks based on detailed biostratigraphic research. He found a disordered and repeated succession of an imbricated mudstone-dominant unit, although he did not describe the geometrical features of out-of-sequence thrusting. DiTullio & Byrne (1990) defined a regional-scale out-of-sequence thrust as a boundary fault between two distinct structural domains and considered it to be rooted in a basal décollement zone. The Inuyama Sequence provides the following features of out-of-sequence thrusting: (1) out-of-sequence thrusts appear to have rooted into a basal décollement, because the basal parts of thrust sheets are commonly marked by the lowest stratigraphic horizon. The geometry of thrust sheets illustrated in Fig. 17 suggests that (2) out-of-sequence thrusts followed in-sequence thrusts locally, and (3) they developed sequentially seaward.

In summary we infer a four-stage sequence of deformation for the evolution of this accretionary wedge (Fig. 18). (1) Seaward of the deformation front, a décollement was initiated within the siliceous mudstone interval. Sand intrusions were tectonically generated in the lower mudstone interval and intruded downward into the boundary region between the ribbon chert and the siliceous mudstone. (2) The stratigraphic section above the décollement was imbricated by in-sequence thrusting in the frontal part of the wedge. This initial stage of thrusting and imbrication was followed by (3) the formation of duplex structures with fault-related folds within the lower stratigraphic section as the décollement stepped down-section to the lowest siliceous claystone interval. Finally, (4) these thrust packages were overprinted by secondary prism thickening in the form of out-of-sequence thrusting.

CONCLUSIONS

(1) The Inuyama Sequence, a Jurassic coherent chert–clastic complex in a part of the Jurassic Mino–Tamba Belt, is characterized by a series of stacked thrust sheets consisting of an Early Triassic to Middle Jurassic oceanic plate stratigraphic succession.

(2) The geometric pattern of the thrust sheets defines a S-verging imbricate fan system. Each thrust sheet is subdivided into two lithotectonic units separated by a intrasheet detachment zone within the siliceous mudstone interval.

(3) F_1 folds in ribbon chert, which are closely related to thrusting, were developed during the diagenetic stage in which ribbon chert was still interbedded CT-chert and CT-porcelanite.

(4) The structural evolution of the Inuyama Sequence is characterized by an offscraping accretionary process

followed by down-stepping of the décollement and out-of-sequence thrusting.

Acknowledgements—We thank Tsunemasa Shiki (Kyoto University), Hiroyuki Suzuki (Doshisha University), Thomas H. Wilson (West Virginia University), Hirokazu Kato (Geological Survey of Japan) and Keiji Nakazawa (Kinki University) for many helpful discussions and for comments on an earlier version of the manuscript, and Koichi Nakamura (Geological Survey of Japan) for advice on thrusts systems. We also thank the Journal reviewers, Mike Underwood and Tim Byrne and the Associate Editor, Peter Hudleston for constructive comments and substantial improvements to our English.

REFERENCES

Adachi, M. 1988. Further study on the Sakahogi conglomerate and surrounding Mesozoic strata in the southern Mino Terrane, Japan. *Bull. Mizunami Fossil Mus.* **14**, 113–128.*

Aoki, Y. T., Tamano, T. & Kato, S. 1983. Detailed structure of the Nankai Trough from migrated seismic sections. In: *Studies in Continental Margin Geology* (edited by Watkins, J. S. & Drake, C. L.). *Mem. Am. Ass. Petrol. Geol.* **34**, 309–322.

Aubouin, J., Bourgois, J. & Azema, J. 1984. A new type of active margin: The convergent–extensional margin, as exemplified by the Middle America Trench off Guatemala. *Earth Planet. Sci. Lett.* **67**, 211–218.

Behrmann, J. H., Brown, K. M., Moore, J. C., Mascle, A. & Taylor, E. *et al.* 1988. Evolution of structures and fabrics in the Barbados Accretionary Prism. Insights from Leg 110 of the Ocean Drilling Program. *J. Struct. Geol.* **10**, 577–591.

Brown, K. M. & Behrmann, J. H. 1990. Genesis and evolution of small-scale structures in the toe of the Barbados ridge accretionary wedge. *Proc. ODP, Sci. Results* **110**, 229–244.

Brueckner, H. K. & Snyder, W. S. 1985. Structure of the Havallah sequence allochthon, Nevada: evidence for prolonged evolution in an accretionary prism. *Bull. geol. Soc. Am.* **96**, 1113–1130.

Brueckner, H. K., Snyder, W. S. & Boudreau, M. 1987. Diagenetic controls on the structural evolution of siliceous sediments in the Golconda allochthon, Nevada, U.S.A. *J. Struct. Geol.* **9**, 403–417.

Coward, M. P. 1980. The Caledonian thrust and shear zones of N.W. Scotland. *J. Struct. Geol.* **2**, 11–17.

DiTullio, L. & Byrne, T. 1990. Deformation paths in the shallow levels of an accretionary prism: the Eocene Shimanto belt of southwest Japan. *Bull. geol. Soc. Am.* **102**, 1420–1438.

Hara, I., Hide, K., Takeda, K., Tsukuda, E., Tokuda, M. & Shiota, T. 1977. Tectonic movement in the Sambagawa belt. In: *The Sambagawa Belt* (edited by Hide, K.). Hiroshima University Press, Hiroshima, 307–390.*

Harm, J. C. 1965. Sandstone dikes in relation to Laramide faults and stress distribution in the southern Front Range, Colorado. *Bull. geol. Soc. Am.* **76**, 981–1002.

Hashimoto, M. & Saito, Y. 1970. Metamorphism of Paleozoic greenstones of the Tamba Plateau, Kyoto prefecture. *J. geol. Soc. Japan* **76**, 1–6.

Hilde, T. W. C. 1983. Sediment subduction versus accretion around the Pacific. *Tectonophysics* **99**, 381–397.

Hori, R. 1986. Parahsuum simplum Assemblage (Early Jurassic radiolarian assemblage) in the Inuyama area, central Japan. *News Osaka Micropaleontol.* **7**, 45–52.*

Hori, R. 1988. Some characteristic radiolarians from Lower Jurassic bedded cherts of the Inuyama area, southwest Japan. *Trans. Proc. Palaeont. Soc. Japan, New Ser.* **151**, 543–563.

Hori, R. 1990. Lower Jurassic radiolarian zones of southwest Japan. *Trans. Proc. Paleont. Soc. Japan, New Ser.* **159**, 562–586.

Isaacs, C. M. 1981. Porosity reduction during diagenesis of the Monterey formation, Santa Barbara coastal area, California. In: *The Monterey Formation and Related Siliceous Rocks of California* (edited by Garrison, R. E. & Douglass, R. G.). *Spec. Publ. Soc. econ. Paleont. Mineral.*, 257–271.

Kagami, H., Shiono, K. & Taira. A. 1985. Subduction of plate at the Nankai Trough and formation of accretionary prism. *Kagaku* **51**, 429–438.†

Kido, S. 1982. Occurrence of Triassic chert and Jurassic siliceous shale at Kamiaso, Gifu Prefecture, central Japan. *News Osaka Micropaleontol.* **5**, 135–151.*

Kondo, N. & Adachi, M. 1975. Mesozoic strata of the area north of Inuyama, with special reference to the Sakahogi conglomerate. *J. geol. Soc. Japan* **81**, 373–386.*

Lash, G. G. 1985. Recognition of trench fill in orogenic flysch sequence. *Geology* **13**, 867–870.

Maruyama, S., Liou, J. G. and Seno, T. 1989. Mesozoic and Cenozoic evolution of Asia. In: *The Evolution of the Pacific Ocean Margins* (edited by Ben-Avraham, Z.). Oxford University Press, New York, 75–99.

Matsuda, T. & Isozaki, Y. 1991. Well-documented travel history of Mesozoic pelagic chert in Japan: from remote ocean to subduction zone. *Tectonics* **10**, 475–499.

Matsuda, T., Isozaki, Y. & Yao, A. 1981. Mode of occurrence of Triassic and Jurassic rocks in Inuyama area, Mino belt. *Proc. Kansai Branch geol. Soc. Japan* **88**,5.†

Matsuoka, A. 1984. Togano group of the Southern Chichibu Terrane in the western part of Kochi Prefecture, Southwest Japan. *J. geol. Soc. Japan* **90**, 455–477.*

Matsushita, S. 1953. *Regional Geology of Japan, Kinkichiho.* Asakura-shoten, Tokyo.†

Miller, E. L., Kanter, L. R., Larue, D. K. & Turner, R. J. 1982. Structural fabric of the Paleozoic Golconda allochthon, Antler Peak quadrangle, Nevada: progressive deformation of an oceanic sedimentary assemblage. *J. geophys. Res.* **87**, 3795–3804.

Mizutani, S. 1964. Superficial folding of the Paleozoic system of central Japan. *J. Earth Sci., Nagoya Univ.* **12**, 17–83.

Mizutani, S. 1977. Progressive ordering of cristobalitic silica in the early stage of diagenesis. *Contr. Miner. Petrol.* **61**, 129–140.

Mizutani, S. & Koike, T. 1982. Radiolarians in the Jurassic siliceous shale and in the Triassic bedded chert of Unuma, Kagamigahara City, Gifu Prefecture, central Japan. *News Osaka Micropaleontol.* **5**, 117–134.*

Moore, G. F., Shipley, T. H., Stoffa, P. L., Karig, D. E., Taira, A., Kuramoto, S., Tokuyama, H. & Suyehiro, K. 1990. Structure of the Nankai Trough accretionary zone from multichannel seismic reflection data. *J. geophys. Res.* **95**, 8753–8765.

Moore, J. C. 1989. Tectonics and hydrogeology of accretionary prisms: role of the décollement zone. *J. Struct. Geol.* **11**, 95–106.

Moore, J. C., Roeske, S., Lundberg, N., Schoonmaker, J., Cowan, D., Gunzales, E. & Lucas, S. 1986. Scaly fabric from Deep Sea Drilling Project cores from forearcs. In: *Structural Fabrics in Deep Sea Drilling Project Cores From Forearcs* (edited by Moore, J. C.). *Mem. geol. Soc. Am.* **166**, 56–73.

Morley, C. K. 1988. Out-of-sequence thrusts. *Tectonics* **7**, 539–561.

Murata, K. J. & Larson, R. R. 1975. Diagenesis of Miocene siliceous shales, Temblor Range, California. *U.S. geol. Surv. J. Res.* **3**, 553–566.

Murchey, B. 1984. Biostratigraphy and lithostratigraphy of chert in the Franciscan complex, Marin Headlands, California. In: *Franciscan Geology of Northern California* (edited by Blake, M. C., Jr). *Spec. Publ. Pacific Sec. Soc. econ. Paleont. Mineral.* **43**, 51–70.

Mutti, E. & Ricci Lucci, F. 1972. Le torbiditi dell'Appennino settentrionale: introduction all'analisi di facies. *Mem. Soc. geol. Ital.* **11**, 161–199.

Nishi, H. 1988. Structural analysis of the Shimanto accretionary complex, Kyushu, Japan, based on foraminiferal biostratigraphy. *Tectonics* **7**, 641–652.

Otsuka, T. 1988. Paleozoic–Mesozoic sedimentary complex in the eastern Mino Terrane, central Japan, and its Jurassic tectonism. *J. Geosci., Osaka City Univ.* **31**, 63–122.

Otsuka, T. 1989. Mesoscopic folds of chert in Triassic–Jurassic chert–clastics sequence in the Mino Terrane, central Japan. *J. geol. Soc. Japan* **95**, 97–111.

Otsuka, T. 1991. Cretaceous left-lateral movement in the Mino Terrane, central Japan. *89th Annu. Meet. geol. Soc. Japan, Abs.*, 319.†

Ramberg, I. B. & Johnson, A. M. 1976. Asymmetric folding in interbedded chert and shale of the Franciscan complex, San Francisco bay area, California. *Tectonophysics* **32**, 295–320.

Ramsay, J. G. 1967. *Folding and Fracturing of Rocks.* McGraw-Hill, New York, 491–496.

Sakaguchi, S. 1961. Stratigraphy and palaeontology of the south Tamba district. Part 1, Stratigraphy. *Mem. Osaka Gakugei Univ.* **10**, 35–76.

Seely, D. R., Vail, P. R. & Walton, G. G. 1974. Trench slope model. In: *The Geology of Continental Margins* (edited by Burk C. A. & Drake C. L.). Springer, New York, 249–260.

Snyder, W. S., Brueckner, H. K. & Schweickert, R. A. 1983. Deformation styles in the Monterey formation and other siliceous sedimentary rocks. In: *Petroleum Generation and Occurrence in the*

Miocene Monterey Formation, California (edited by Isaacs, C. M. & Garrison, R. E.). *Spec. Publ. Pacific Sec. Soc. econ. Paleontol. Mineral.*, 151–170.

Stewart, J. H., Murchey, B., Jones, D. L. & Wardlaw, B. R. 1986. Paleontologic evidence for complex tectonic interlayering of Mississippian to Permian deep-water rocks of the Golconda allochthon in Tobin Range, north-central Nevada. *Bull. geol. Soc. Am.* **97**, 1122–1132.

Taira, A., Saito, Y. & Hashimoto, M. 1983. The role of oblique subduction and strike-slip tectonics in the evolution of Japan. In: *Geodynamics of the Western Pacific–Indonesian Region* (edited by Hilde, T. W. C. & Uyeda, S.). *Am. Geophys. Un. Geodyn. Ser.* **11**, 303–316.

Taira, A., Tokuyama, H. & Soh, W. 1989. Accretion tectonics and evolution of Japan. In: *The Evolution of the Pacific Ocean Margins* (edited by Ben-Avraham Z.). Oxford University Press, New York. 100–123.

Wahrhaftig, C. 1984. Structure of the Marin Headlands block, California: a progress report. In: *Franciscan Geology of Northern California* (edited by Blake M. C., Jr). *Pacific Section Soc. econ. Paleontol. Mineral.* **43**, 31–50.

Wakita, K. 1988. Origin of chaotically mixed rock bodies in the Early Jurassic to Early Cretaceous sedimentary complex of the Mino terrane, central Japan. *Bull. geol. Surv. Japan* **39**, 675–757.

Westbrook, G. K., Mascle, A. & Biju-Duval, B. 1984. Geophysics and structure of the Lesser Antilles forearc. *Init. Reps DSDP*, **78A**, 23–38.

Williams, I. A., Parks, G. A. & Crerar, D. A. 1985. Silica diagenesis, II. General mechanisms. *J. sedim. Petrol.* **55**, 312–321.

Yao, A., Matsuda, T. & Isozaki, Y. 1980. Triassic and Jurassic radiolarians from the Inuyama area, central Japan. *J. Geosci. Osaka City Univ.* **23**, 135–155.

---

*In Japanese with English abstract.

†In Japanese.